Centric Heterochromatin and the Efficiency of Achiasmate Disjunction in *Drosophila* Female Meiosis

Gary H. Karpen,* Mong-Huong Le, Hiep Le

The chromosomal requirements for achiasmate (nonexchange) homolog disjunction in *Drosophila* female meiosis I have been identified with the use of a series of molecularly defined minichromosome deletion derivatives. Efficient disjunction requires 1000 kilobases of overlap in the centric heterochromatin and is not affected by homologous euchromatin or overall size differences. Disjunction efficiency decreases linearly as heterochromatic overlap is reduced from 1000 to 430 kilobases of overlap. Further observations, including rescue experiments with *nod* kinesin-like protein transgenes, demonstrate that heterochromatin does not act solely to promote chromosome movement or spindle attachment. Thus, it is proposed that centric heterochromatin contains multiple pairing elements that act additively to initiate or maintain the proper alignment of achiasmate chromosomes in meiosis I. How heterochromatin could act to promote chromosome pairing is discussed here.

The disjunction of homologous chromosomes during meiosis I ensures that gametes and offspring contain the proper number and types of chromosomes. Errors in meiotic disjunction are a major problem in human populations (*1*). Meiotic disjunction requires multiple steps and mechanisms, including the initiation and maintenance of homolog associations in prophase, prometaphase, and metaphase (pairing) and the subsequent movement of homologous centromeres of each bivalent to opposite poles during anaphase (segregation). In meiosis I, exchange between homologs is usually required to ensure proper disjunction [reviewed in (*2*)]; however, in many organisms nonexchange (achiasmate) chromosome pairs disjoin normally [reviewed in (*3*)]. In *Drosophila* females, nonexchange chromosomes disjoin by means of a backup system originally called "distributive pairing" (*4*). A similar system acts during *Saccharomyces cerevisiae* meiosis, although in many details it differs mechanistically from that in *Drosophila* (*5*, *6*).

How do achiasmate chromosomes pair and segregate in *Drosophila* female meiosis? Grell performed a series of pioneering genetic studies (*4*) and concluded that chromosome size similarity is the basis for achiasmate pairing and segregation. The recent studies by Hawley and colleagues (*7*) led to a different hypothesis, that two achiasmate disjunction systems exist in *Drosophila* females: a "homologous achiasmate system" that relies on heterochromatic homology and a "heterologous system" that balances equal amounts of chromatin across the metaphase I plate. However, the molecular structures of the chromosomes used to assay disjunction in both studies could not be determined. Molecular-genetic dissection of the chromosomal regions involved in achiasmate disjunction is required to directly address a number of important questions. For example, do specific regions of the chromosome act to promote meiotic disjunction or is overall homology or size differential responsible?

Molecular Biology and Virology Laboratory, Salk Institute for Biological Studies, La Jolla, CA 92037, USA.

*To whom correspondence should be addressed. E-mail: karpen@salk.edu

The *Drosophila* minichromosome *Dp(1;f) 1187* (*Dp1187*) has been a useful substrate for molecular-genetic dissections of metazoan chromosome structure and function (*8–10*). For example, full centromere function requires a specific 420-kb region (*11*) of the 1000-kb centric heterochromatin (Fig. 1A). Here, we investigated the chromosomal elements responsible for achiasmate meiotic disjunction in *Drosophila* females by monitoring the genetic disjunction behavior of two homologous minichromosomes of known molecular structure.

Differentially marked full-length *Dp1187* minichromosomes were analyzed to determine the baseline efficiency of minichromosome meiotic disjunction. Animals disomic for a y^+ ry^- (*Dp1187*) and a y^- ry^+ (*γ158*) derivative (Fig. 1A), in addition to the normal chromosome complement, were crossed to y^- ry^- animals, and progeny counts were used to determine the percent nondisjunction [ND, the frequency of the 0 Dp (y− ry−) and 2 Dp (y+ ry+) nondisjunction progeny classes]. Only 5% nondisjunction of two *Dp1187* minichromosomes was observed in females (Fig. 1A), compared to the 50% value expected for random disjunction. In males, the same two *Dp1187* minichromosomes segregated at random [47% ND (*11a*)]. Thus, *Dp1187* contains sequences sufficient to promote homolog disjunction in meiosis I in females but not in males (*12*).

Dp1187 derivatives (rearranged mini-

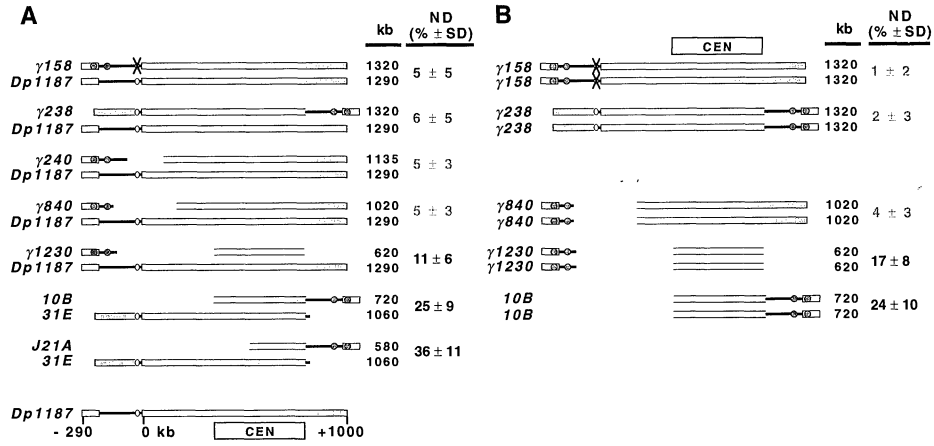

Fig. 1. Meiotic disjunction of *Dp1187* minichromosomes in females. (**A**) Structurally altered minichromosome homologs can display abnormal disjunction. *Dp1187* contains euchromatin (solid line) and subtelomeric heterochromatin (gray box); the 1 Mb of centric heterochromatin is shown as a box with a gray gradient (0 to +1000 kb), and the location of the fully functional centromere (CEN) is shown. Minichromosomes (overall sizes indicated in kilobases) are marked with the *yellow*$^+$ (y^+) body color gene (open oval) or two *rosy*$^+$ (ry^+) eye color genes inserted by P element transposition (dark gray circles) (*58*). *γ158* contains a point mutation in the *yellow* gene (y^-) (*10*, *59*). The disjunction behavior of different minichromosomes was determined as described in the text and in (*56*). Nondisjunction (ND) frequencies (reported as % ND ± SD) (*57*) that were not significantly different from control values (*γ158/Dp1187*) are shown in gray, whereas those that differed significantly from controls are shown in black ($P < 0.05$, t test) (*57*). (**B**) Size similarity does not ensure normal disjunction. The disjunction behavior of identical and same-size partners was determined (*60*); numbers in black are significantly different from control values (*γ158/γ158*). Comparison to the behavior of the same chromosomes with structurally different derivatives [as shown in (A)] demonstrates that structural homology and organization are the primary determinants of disjunction efficiency, rather than size similarity.

chromosomes with molecularly defined inversions or deletions) (*10*, *11*) provide a powerful resource for mapping the chromosomal elements responsible for homolog disjunction during female meiosis and for testing the role of similar partner size in the achiasmate system (*13*). Animals disomic for differentially marked derivatives (y+ ry− and y− ry+) were generated as before, then outcrossed to measure their disjunction efficiency. A number of inversion and deletion derivatives [γ*238* (1320 kb), γ*240* (1115 kb), and γ*840* (1020 kb)] (Fig. 1A) segregated normally from full-length *Dp1187* partners (1290 kb). Therefore, deleting up to 270 kb of euchromatin and heterochromatin did not have a significant effect on disjunction efficiency. In contrast, γ*1230* (620 kb) displayed twofold higher nondisjunction from *Dp1187* (11%) than the rate observed in controls (γ*158*/*Dp1187*, 5%), *10B* (720 kb), and *31E* (1060 kb) nondisjoined in 25% of meioses, and *J21A* (580 kb) segregated very poorly from *31E* (36% ND). We conclude that large structural rearrangements can affect *Dp1187* achiasmate disjunction dramatically and that the magnitude of the disjunction defect is positively correlated with the size of the deletion.

The abnormal disjunction of structurally rearranged *Dp1187* partners could be caused by size differences or by alteration of specific chromosomal regions required for pairing or subsequent segregation. The partners that displayed the most defective disjunction behavior differed greatly in size (1290 versus 620 kb for *Dp1187*/γ*1230*, and 1060 versus 580 kb for *31E*/*J21A*) (Fig. 1A). If disjunction of achiasmate chromosomes depends only on size similarity, as proposed by Grell (*4*), then abnormal disjunction should be rescued by placement of the smaller partner with a chromosome of similar size. Instead, we observed that γ*1230*/γ*1230* disjunction (17% ND; Fig. 1B) was less than γ*1230*/*Dp1187* disjunction (11% ND), and *10B*/*10B* disjunction (24% ND) was not significantly greater than that in *10B*/*31E* (25% ND) (*14*). We conclude that the severely abnormal disjunctions of γ*1230*/*Dp1187*, *10B*/*31E* and *J21A*/*31E* are not caused by the dissimilar sizes of the partners and that size similarity is not an important determinant of *Dp1187* achiasmate disjunction.

Does normal disjunction require that genetic partners are homologous in chromosome structure and composition? Our data (Fig. 1) suggest that at least two regions of *Dp1187* heterochromatin (+150 to +580 and +580 to +1000) must be present for proper pairing or segregation (*15*). Finer resolution mapping of achiasmate disjunction elements was accomplished with analyses of the terminally deficient $y^- ry^+$ γ*238* derivatives (Fig. 2A) (*11*), which represent a series of chromosomes that differ only in the amount of centric heterochromatin shared with the common *31E* partner ($y^+ ry^-$). Genetic analyses of γ*238* derivative disomes indicated that the efficiency of meiotic disjunction depends directly on the amount of centric heterochromatin overlap between partners (Fig. 2A). Roughly 1000 kb of centric heterochromatin overlap produced efficient disjunction (γ*238*/*31E*, 6% ND), whereas less than 390 kb resulted in very poor disjunction (*J21A*/*31E*, 36% ND). The correlation between heterochromatic overlap and disjunction efficiency was nearly linear from 430 to 1000 kb of overlap (Fig. 2B, region 1). Below 430 kb, the relation between overlap and disjunction efficiency is more complex (regions 2 and 3). Perhaps a threshold for disjunction is reached between 390 and 430 kb of overlap (region 3) or this region of the minichromosome is particularly effective at promoting disjunction (see below).

Surprisingly, euchromatin and subtelomeric heterochromatin are not substantial contributors to *Dp1187* disjunction. *10B* and *31E* lack significant overlap in the euchromatin and subtelomeric heterochromatin and have only 430 kb of centric heterochromatin overlap (Fig. 1A). In comparison, *10B*/*10B* partners contain an additional 290 kb of homologous euchromatin and subtelomeric heterochromatin yet display no increase in disjunction efficiency (Fig. 1B). However, addition of a similar amount of homologous centric heterochromatin (270 kb) decreased nondisjunction significantly (compare *30A*/*31E* to *10B*/*31E*) (Fig. 2A). We conclude that euchromatic and subtelomeric regions have no significant effect on achiasmate disjunction of *Dp1187* in female meiosis, in comparison to the major contribution of centric heterochromatin overlap. These results are consistent with the suggestion of Hawley *et al.* (*7*) that achiasmate disjunction of homologous chromosomes requires centric heterochromatin.

Centric heterochromatin could promote meiosis I disjunction by initiating or maintaining chromosome pairing during prophase or metaphase, or by ensuring normal segregation during anaphase. Heterochromatin clearly plays an important role in the physical movement of chromosomes in mitosis and meiosis. Centromeres are present in heterochromatin and are required for kinetochore formation, sister chromatid cohesion, attachment to the spindle, and chromosome movement (*16*). In addition, the NOD protein [a "chromokinesin" that binds DNA (*17*)] ensures normal transmission and disjunction by interacting with euchromatic and heterochromatic regions that lie outside the centromere (*18*). NOD promotes chromosome segregation, most likely by providing an anti-poleward force necessary to maintain spindle-kinetochore interactions (*17*, *18*).

The sensitivity of *Dp1187* deletion derivatives to *nod* gene dosage (*18*) suggests a plausible explanation for their nondisjunction: deletion of minichromosomal nod^+ interaction regions could result in abnormal anaphase segregation, despite the presence of two normal copies of nod^+. We tested this hypothesis by seeing whether extra copies of the nod^+ gene could rescue the abnormal disjunction of *Dp1187* derivatives (Fig. 3). One or two extra copies of the transgene (T), in addition to the two endogenous copies of nod^+ (E), had no significant effect on abnormal disjunction for any of the partners. For example, the poor disjunction of *J21A*/*31E* (2E+0T, 36%) remained high in 2E+1T (34%) and 2E+2T (35%) combinations (Fig. 3). The activity of this transgene was demonstrated previously by its ability to rescue 4th chromosome disjunction defects in *nod*/*nod* homozygotes (*19*); in our studies,

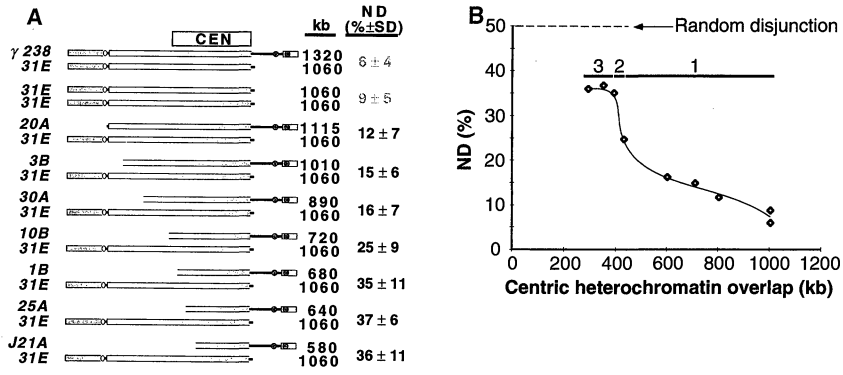

Fig. 2. Achiasmate disjunction is correlated with the amount of centric heterochromatin overlap. (**A**) Disjunction analysis of a series of γ*238* derivatives. Fine-resolution mapping of disjunction elements was performed with the γ*238* terminal deficiency derivatives shown. Numbers in black are significantly different from control values (γ*238*/*31E*). (**B**) Graph of heterochromatic overlap versus disjunction efficiency. For the γ*238* derivatives shown in (A), the percent nondisjunction (ND) is plotted against the amount of centric heterochromatin overlap.

the *nod*$^+$ transgene was able to rescue *J21A* monosome transmission (2E+0T, 24%, versus 2E+2T, 36%) (Fig. 3). Therefore, defective *Dp1187* disjunction is not caused by failures in *nod*-dependent segregation.

Other observations argue persuasively against the hypothesis that *Dp1187* centric heterochromatic deletions disrupt disjunction only by interfering with chromosome movement and strongly support a role for heterochromatin in the physical pairing of homologs. First, meiotic disjunction and segregation require different amounts and regions of the centric heterochromatin. The presence of sequences sufficient to promote normal centromere function—specifically the 420 kb present in *10B* and *γ1230* (CEN; Fig. 1A)—does not guarantee normal disjunction. Normal meiotic pairing requires 1000 kb of heterochromatin, which includes extensive regions that lie outside the centromere. Second, abnormal chromosome movement would cause chromosome loss in addition to pure nondisjunction, resulting in an overrepresentation of the nullosomic (0 Dp) over the disomic (2 Dp) nondisjunction classes. In our studies, the 0 Dp and 2 Dp classes were equally represented, even when partners displayed high rates of nondisjunction (*20*).

Independent cytological studies demonstrate that heterochromatic regions are physically associated during female meiosis. Electron microscopic analyses (*21*, *22*) indicate that heterochromatic regions are paired during pachytene. Recent in situ hybridization studies of oocyte nuclei, using satellite DNA probes and highly sensitive fluorescence microscopy, demonstrate that heterochromatic regions of homologous achiasmate chromosomes are tightly associated before segregation (*23*). Our molecular-genetic analyses, combined with these cytological observations, strongly support the conclusion that centric heterochromatin ensures disjunction by mediating chromosome pairing. This pairing function is distinct from, and in addition to, the important roles of centric heterochromatin in subsequent segregation.

Heterochromatin is an enigmatic component of multicellular eukaryotic genomes; it is distinguishable from euchromatin because it is sparsely populated with genes, inhibits the function of euchromatic genes (position-effect variegation), replicates late in the S phase, and is rich in tandemly repeated "satellite" sequences (*24*, *25*). What is the nature of the heterochromatic sequences that contribute to achiasmate pairing? The regions of *Dp1187* that function in this process contain diverse sequence elements, including different satellite arrays and transposable elements (*10*, *26*). Disjunction efficiency responds linearly to small additions of this heterochromatin (region 1; Fig. 2B), which suggests that *Dp1187* heterochromatin does not contain one or a few specific pairing sites. Rather, we conclude that centric heterochromatin contains multiple pairing elements that act additively to initiate or maintain the proper alignment of achiasmate chromosomes early in meiosis I.

Interestingly, partners with <430 kb of heterochromatic homology deviated from the linear response and displayed very low disjunction efficiencies (regions 2 and 3, Fig. 2B). This behavior is specifically associated with breakpoints in or near the minimal functional centromere (*11*). Perhaps the macromolecular kinetochore structure or sister chromatid cohesion proteins associated with the centromere (*16*) interfere with the ability of nearby heterochromatic regions to promote pairing (region 2), while still providing residual pairing activity that ensures some disjunction (region 3).

There are at least three general molecular mechanisms that explain how multiple domains within heterochromatin might promote achiasmate meiotic pairing and homolog recognition. First, achiasmate pairing could occur by means of a DNA homology search mechanism. Heterochromatic homology could be determined by base pairing between potential partners, similar to recombination pairing (*27*–*29*). However, heterochromatic regions display severely repressed reciprocal recombination frequencies (*30*–*32*) and are likely excluded from base pair homology searches. In addition, most heterochromatic repeats (simple and complex satellites and transposable elements) are not specific to a particular chromosome (*10*, *33*, *34*); extensive regions (hundreds or thousands of kilobases) of identity or near identity between "nonhomologous" chromosomes would likely confuse a general base pair homology search.

Second, partner recognition and pairing could be mediated by special pairing proteins or complexes that interact with identical sequences present on both homologs. In this model, homolog recognition would depend on the arrangement of heterochromatic sequences and their corresponding pairing proteins (a combinatorial mechanism) to circumvent the problems posed by heterochromatic sequence identities present in "nonhomologous" partners. This model would be supported by the identification of genes and proteins that are specific to and essential for achiasmate pairing.

Third, pairing could be accomplished by intrinsic heterochromatic features or proteins that are not solely dedicated to meiotic pairing. Multimeric complexes appear to participate in heterochromatin-induced position-effect variegation (gene silencing) in somatic cells [reviewed in (*24*, *25*, *35*)]. Cross-multimerization of such proteins, in this case between homologs, could be coopted to promote physical associations during meiosis, and pairing specificity could be provided by the combinatorial action of

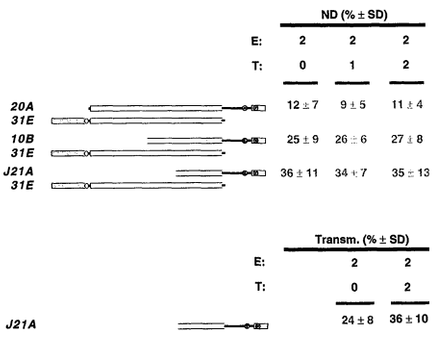

Fig. 3. Extra copies of the *nod*$^+$ kinesin-like gene rescues unstable transmission but does not rescue abnormal disjunction. Animals carrying two copies of the endogenous *nod*$^+$ gene (E) and zero, one, or two copies of a *nod*$^+$ transgene (T) were analyzed for *J21A* monosome transmission (bottom) and meiotic disjunction of the partners shown (top) (*61*). Two copies of the transgene raised *J21A* transmission significantly (36%, black), in comparison to controls (24%). In contrast, abnormal meiotic disjunction of the partners shown was not rescued by having one or two additional copies of the *nod*$^+$ transgene.

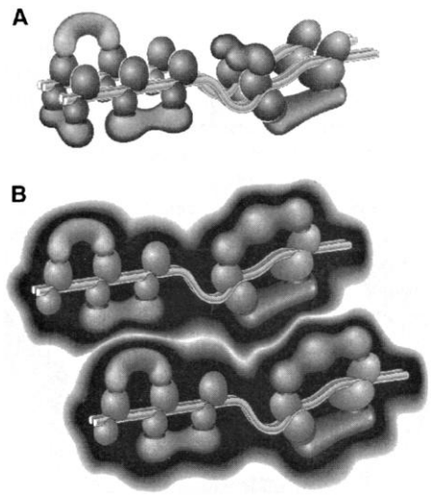

Fig. 4. Meiotic pairing as an intrinsic property of heterochromatin. (**A**) Cross-homolog multimerization. Multimerization complexes that normally form within the heterochromatin to promote intrinsic heterochromatic functions, such as sister chromatid cohesion, kinetochore formation, or chromatin structure, could also form between homologs, providing both pairing specificity and direct physical contact in meiosis. Double bars represent sister chromatids. (**B**) Heterochromatic landscape "fit." DNA and protein structures inherent to heterochromatin could produce a self-complementary chromosome "landscape" (black background), which ensures partner recognition and alignment by a "best fit" mechanism. Double bars represent sister chromatids.

different complexes (Fig. 4A). Alternatively, a series of proteins that normally bind to heterochromatin, or higher order structures inherent to the DNA sequences, could create a "landscape" that facilitates homolog recognition by a "best fit" mechanism (Fig. 4B). The sequence composition of centric heterochromatin [long stretches of satellite DNA broken up by complex DNAs, such as transposable elements (*10*, *33*, *34*)] lends itself to the creation of distinct and unusual higher order structures, such as DNA bending (*36*, *37*).

The idea that intrinsic structural and functional properties of the heterochromatin provide the physical basis for pairing is attractive, because no novel components or mechanisms are required and it readily explains why heterochromatin, rather than euchromatin, is used for achiasmate pairing. Furthermore, these types of heterochromatic interactions do not have to arise during meiosis; they could carry over from heterochromatic associations intrinsic to premeiotic mitotic cells, visualized cytologically as somatic pairing (*38*, *39*) and the Rabl orientation (*40*, *41*). Both versions of this model predict that abnormal achiasmate pairing would be caused by mutations in gene products that play general roles in heterochromatin metabolism or function, including kinetochore components (*16*), sister chromatid cohesion proteins (*42*, *43*), and heterochromatic proteins involved in chromatin structure or position-effect variegation (*25*, *44*, *45*). These classes of proteins would not be expected to contribute to meiotic pairing in the DNA homology and specialized pairing protein models.

The results presented here, combined with the recent studies of Dernburg *et al.* (*23*), provide strong molecular-genetic and physical evidence that heterochromatin plays an important role in achiasmate meiotic pairing in *Drosophila* females. Further investigations of the cis and trans components involved in achiasmate disjunction are necessary to test specific predictions of the models presented here. Studies of the proteins involved directly in initiating or maintaining achiasmate pairing will determine how heterochromatin promotes homolog recognition at the molecular level and why centric heterochromatin is responsible for this essential biological function.

REFERENCES AND NOTES

1. T. Hassold, P. A. Hunt, S. Sherman, *Curr. Opin. Genet. Dev.* **3**, 398 (1993).
2. R. S. Hawley, K. S. McKim, T. Arbel, *Annu. Rev. Genet.* **27**, 281 (1993).
3. K. W. Wolf, *Bioessays* **16**, 107 (1994).
4. R. F. Grell, in *The Genetics and Biology of* Drosophila, M. Ashburner and E. Novitski, Eds. (Academic Press, London, 1976), vol. 1a, pp. 435–486.
5. J. Loidl, H. Scherthan, D. B. Kaback, *Proc. Natl. Acad. Sci. U.S.A.* **91**, 331 (1994).
6. L. O. Ross, S. Rankin, M. F. Shuster, D. S. Dawson, *Genetics* **142**, 79 (1996).
7. R. S. Hawley *et al.*, *Dev. Genet.* **13**, 440 (1993).
8. G. H. Karpen and A. C. Spradling, *Cell* **63**, 97 (1990).
9. ———, *Genetics* **132**, 737 (1992).
10. M. H. Le, D. Duricka, G. H. Karpen, *ibid.* **141**, 283 (1995).
11. T. D. Murphy and G. H. Karpen, *Cell* **82**, 599 (1995).

11a. G. H. Karpen, data not shown.

12. Random disjunction of these minichromosomes in males is most likely explained by the fact that *Dp1187*, which is derived from the X chromosome (*8*), does not contain the normal X-Y pairing site (ribosomal DNA) (*46*, *47*).
13. *Drosophila* females use an achiasmate disjunction system to disjoin *Dp1187* homologs. First, the minichromosome is derived from two regions that normally exhibit very few reciprocal exchanges (the X tip and the X centric heterochromatin) (*31*), and as expected there is no observed recombination between *Dp1187* homologs (*48*). Second, *Dp1187* transmission and segregation are altered (*18*, *49*) in animals that contain mutations that predominantly affect achiasmate chromosomes [for example, *nod* and *ncd* (*50*, *51*)]. Third, *Dp1187* homologs are positioned between the metaphase plate and the poles (*52*), a cytological characteristic of achiasmate chromosomes (*53*).
14. Note that the greater disjunction of *γ238/γ238* and *γ158/γ158* (1 and 2% ND, respectively; Fig. 1B) in comparison to that for *γ158 /Dp1187* and *γ238/ Dp1187* (5 and 6% ND, respectively; Fig. 1A) makes the lack of improvement seen for *10B/10B* and *γ1230/γ1230* even more significant.
15. The +150 to +580 disjunction element is defined by the difference between the *γ840* (normal disjunction) and *γ1230* (abnormal disjunction) breakpoints. The +580 to +1000 region must contain significant disjunction function, because the observed 11% nondisjunction of *γ1230* from *Dp1187* is substantially less than the 50% expected for random disjunction.
16. A. F. Pluta, A. M. Mackay, A. M. Ainsztein, I. G. Goldberg, W. C. Earnshaw, *Science* **270**, 1591 (1995).
17. K. Afshar, N. R. Barton, R. S. Hawley, L. S. B. Goldstein, *Cell* **81**, 129 (1995).
18. T. D. Murphy and G. H. Karpen, *ibid.*, p. 139.
19. K. Afshar, J. Scholey, R. S. Hawley, *J. Cell. Biol.* **131**, 833 (1995).
20. For example, *30A/31E* females (Fig. 2A) produced 8.7% y− ry+ progeny (0 Dp nondisjunction class) and 8.2% y+ ry+ progeny (2 Dp nondisjunction class); these values are not statistically different (two-tailed *t* test assuming unequal variances, $t = 0.73$). Similar results were obtained with other combinations of stably transmitted but aberrantly disjoining chromosomes.
21. A. T. Carpenter, *Chromosoma* **51**, 157 (1975).
22. ———, *Genetics* **92**, 511 (1979).
23. A. F. Dernburg, J. W. Sedat, R. S. Hawley, *Cell*, in press.
24. K. S. Weiler and B. T. Wakimoto, *Annu. Rev. Genet.* **29**, 577 (1995).
25. G. H. Karpen, *Curr. Opin. Genet. Dev.* **4**, 281 (1994).
26. X. Sun, J. Wahlstrom, G. H. Karpen, unpublished results.
27. N. Kleckner and B. M. Weiner, *Cold Spring Harbor Symp. Quant. Biol.* **58**, 553 (1993).
28. B. M. Weiner and N. Kleckner, *Cell* **77**, 977 (1994).
29. P. B. Moens, *Bioessays* **16**, 101 (1994).
30. G. Wurglics and H. J. Becker, *Naturwissenschaften* **80**, 174 (1993).
31. M. Ashburner, Drosophila: *A Laboratory Handbook* (Cold Spring Harbor Press, Cold Spring Harbor, NY, 1990).
32. E. L. Cabot, P. Doshi, M. L. Wu, C. I. Wu, *Genetics* **135**, 477 (1993).
33. A. R. Lohe, A. J. Hilliker, P. A. Roberts, *ibid.* **134**, 1149 (1993).
34. S. Pimpinelli *et al.*, *Proc. Natl. Acad. Sci. U.S.A.* **92**, 3804 (1995).
35. V. Orlando and R. Paro, *Curr. Opin. Genet. Dev.* **5**, 174 (1995).
36. R. Benfante, N. Landsberger, D. Maiorano, G. Badaracco, *Gene* **94**, 217 (1990).
37. R. K. Niedenthal, G. M. Sen, A. Wilmen, J. H. Hegemann, *Nucleic Acids Res.* **21**, 4726 (1993).
38. A. K. Csink and S. Henikoff *Nature* **381**, 529 (1996); A. F. Dernburg *et al.*, *Cell* **85**, 745 (1996).
39. Y. Hiraoka *et al.*, *J. Cell Biol.* **120**, 591 (1993).
40. C. Rabl, *Morphologisches Jarbuch* **10**, 214 (1885).
41. M. Hochstrasser, D. Mathog, Y. Gruenbaum, H. Saumweber, J. Sedat, *J. Cell Biol.* **102**, 112 (1986).
42. W. Miyazaki and T. Orr-Weaver, *Annu. Rev. Genet.* **28**, 167 (1994).
43. A. W. Kerrebrock, D. P. Moore, J. S. Wu, T. L. Orr-Weaver, *Cell* **83**, 247 (1995).
44. T. Grigliatti, *Methods Cell Biol.* **35**, 587 (1991).
45. G. Reuter and P. Spierer, *Bioessays* **14**, 605 (1992).
46. B. D. McKee and G. H. Karpen, *Cell* **61**, 61 (1990).
47. B. D. McKee, L. Habera, J. A. Vrana, *Genetics* **132**, 529 (1992).
48. G. H. Karpen, unpublished data.
49. K. Cook, T. D. Murphy, T. Nguyen, G. H. Karpen, unpublished results.
50. S. A. Endow, S. Henikoff, L. Soler-Niedziela, *Nature* **345**, 81 (1990).
51. P. Zhang, B. A. Knowles, L. S. Goldstein, R. S. Hawley, *Cell* **62**, 1053 (1990).
52. K. Yook, G. H. Karpen, W. Sullivan, unpublished results.
53. W. E. Theurkauf and R. S. Hawley, *J. Cell Biol.* **118**, 759 (1992).
54. D. L. Lindsley and G. G. Zimm, *The Genome of* Drosophila melanogaster (Academic Press, New York, 1992).
55. J. Tower, G. H. Karpen, N. Craig, A. C. Spradling, *Genetics* **133**, 347 (1993).
56. All minichromosome stocks were crossed into a y^1 ; ry^{506} background. Disomic animals (*Dp1187/γ158*) were produced by crossing *y/y*; *ry/ry*; *Dp1187*, y^+ ry^- (y+ ry−) females to *y/Y*; *ry/ry*; *γ158*, y^- ry^+ (y− ry+) males. The y+ ry+ phenotype distinguished the *Dp1187/γ158* disomic animals from F_1 siblings monosomic (y− ry+ and y+ ry−) or nullosomic (y− ry−) for these minichromosomes. Meiotic disjunction behavior was determined by crossing individual females containing two minichromosomes to three *X^Y*, *y/0*; ry^{506} males, in vials. The compound X-Y chromosome *YSX.YL, In(1)EN, y* (*54*) (referred to here as *X^Y*) was used to suppress variegation of the y^+ and ry^+ genes observed in some *Dp1187* derivatives (*10*, *11*, *18*). This cross produces both *X/X^Y* and *X/O* progeny, but *X/O* males were not scored, because of their enhanced variegation.
57. The true nondisjunction rate (TND) corrected for chromosome loss was calculated for each female with the formula 50% × [frequency y+ ry+/(frequency y+ × frequency ry+)], as described previously (*18*). The numerator in the TND calculation is the observed frequency of progeny receiving both minichromosomes (unequivocal nondisjunction events, 2 Dp class; Fig. 1B); the denominator is the frequency of both minichromosomes segregating independently. This ratio will equal 1 if disjunction occurs at random; it is multiplied by 50% to specify random disjunction as 50%. It is important to note that the TND is identical to the standard ND frequency [100% × (exceptions/total)] for all cases except disjunction tests involving the partially unstable chromosomes *J21A*, *25A*, and *1B*; all data are presented as TND merely for consistency. The overall frequencies of y+ or ry+ progeny reflect the transmission rates of each minichromosome. All transmission and nondisjunction frequencies were measured in at least two independent experiments and reproduced to within 5% in all cases. Between 11 and 46 individual females were crossed in each experiment, and an average of 92 progeny per female were scored. Statistical tests (*t* tests) were performed as described (*11*, *18*); only differences associated with *P* values less than 0.05 were considered significant.
58. The generation and structure of *Dp1187* (*8*) and its derivatives are described in previous publications. The γ symbol indicates gamma irradiation–induced derivatives of *Dp8-23* (*10*); *Dp8-23* contains two $rosy^+$ (ry^+) P element insertions at −246 and −185 (*9*, *55*). *31E*, *20A*, *3B*, *30A*, *10B*, *1B*, *25A*, and *J21A*

are terminal deletion derivatives of the γ*238* inversion (*11*).

59. K. D. Donaldson and G. H. Karpen, unpublished results.
60. In cases where partners were marked with the same genetic marker (most of Fig. 2B), disomic animals could not be positively identified in the F_1 generation. Therefore, in each experiment a large number (*30*) of randomly selected ry+ or y+ F_1 progeny (which includes both 1 Dp and 2 Dp animals) were outcrossed to *X^Y, y/0; ry*^{506} males. The 2 Dp F_1 animals used to estimate disjunction frequencies were identified by observation of high transmission rates in the F_2 scoring generation. Nondisjunction rates were calculated as above, except that the nondisjunction class was determined by doubling the number of 0 Dp animals in the F_2 generation. This correction was necessary because the 2 Dp nondisjunction progeny could not be distinguished phenotypically from the 1 Dp class in these crosses. The fact that recovery of the 0 Dp and 2 Dp classes did not differ significantly when both classes could be monitored independently strongly validates the use of this correction. Furthermore, outcrossing the F_2 ry+ progeny from putative *γ1230/γ1230* F_1 animals demonstrated that the F_2 progeny contained equal numbers of 0 Dp and 2 Dp animals (G. H. Karpen *et al.*, data not shown). This result confirmed both the disomic nature of the F_1 parents and the appropriateness of using the 0 Dp class to estimate nondisjunction.
61. Animals with two differentially marked minichromosomes and zero, one, or two copies of the *P(nod*$^+$*)* transgene (*19*) were generated from the cross *y ; P(nod*$^+$*)/SM1, Cy ; ry ; 31E, y*$^+$ females x *y/*Y ; *P(nod*$^+$*)/Sp ; ry ; J21A, ry*$^+$ males (or *20A* or *10B*). The *y ; P(nod*$^+$*)/Sp; ry* female progeny provided the 2E+1T class, and the 2E+2T females were the *y; P(nod*$^+$*)/P(nod*$^+$*); ry* siblings. The *J21A* monosome siblings (y− ry+) were used for the transmission tests, whereas the *31E/J21A*, *31E/10B*, and *31E/20A* disomes (y+ ry+) were used in the nondisjunction tests. The 2E+0T control ND frequencies were taken from the data in Fig. 2A, because independent analyses demonstrated that the SM1 balancer raises nondisjunction frequencies significantly. For the *J21A* monosome transmission tests, the 2E+0T class used in the transmission assay were produced by the cross *y; ry; J21A, ry*$^+$ females x *y/*Y; *P(nod*$^+$*)/*Sp ; *ry* males. All test females were crossed and the results analyzed as described (*56, 57*).
62. T. Murphy contributed significantly to discussions and data analyses, and his efforts are gratefully acknowledged. We also thank K. Cook, R. Kolodner, T. Murphy, and D. Weigel for comments on the manuscript, K. Afshar and R. S. Hawley for the *nod*$^+$ transgene stock (placW nod$^+$-15), J. Simon for the artwork in Fig. 4, and A. Dernburg, J. Sedat, and S. Hawley for communicating results before publication. This research was supported by a grant from the American Cancer Society (DB-1200), which we gratefully acknowledge.

23 May 1996; accepted 10 June 1996

TECHNICAL COMMENTS

Miocene Deposits in the Amazonian Foreland Basin

In their report, Matti E. Räsänen *et al.* state that there is a tidal origin for the sedimentary sequences they studied in the western Amazon region (*1*). Their interpretation of these sequences in Acre, Brazil, as tidal, on the basis of a relatively small data set, implies the existence of a marine connection between the Caribbean Sea and the southern Atlantic Ocean. Background information and earlier work suggests that this conclusion is not the best explanation of the sediments in Acre. The sedimentary history and paleogeography of this area are more complex than Räsänen *et al.* or S. David Webb, in his Perspective (*2*), suggest.

The outcrops studied by Räsänen *et al.* represent a small (areal) part of the Miocene stratigraphic level. The Solimões Formation (also Pebas Formation), to which these sediments belong, crops out in a vast area of Brazilian, Peruvian, and Colombian Amazonia. This formation is up to 980 meters thick and is part of the infill of several sedimentary basins. In the last 20 years, extensive geological studies (*3–10*) have shown that the Solimões Formation was mainly formed in a fluvio-lacustrine system of Andean origin, which was periodically affected by marine ingressions. This fluvio-lacustrine system originated during the Middle Miocene as a result of the uplift of the Eastern Cordillera, and was the ancestor of the present Amazon River. Contrary to what Webb suggests (*2*), "substantial evidence" concerning the marine influence during the Miocene in the area was published (*7–10*) before the Räsänen *et al.* report appeared.

The changes in drainage patterns caused by the genesis of the paleo–Amazon River system and the abortion of the previously existing east-to-west–directed fluvial system had a major influence on the development of the ecosystem, the sedimentary history, and the paleogeography of Amazonia (*8–11*). Subsequently, when establishing a paleogeographic model for the Miocene history of Amazonia, both the fluvial dynamics as well as the tidal influence and marine ingressions should be included. Therefore, Webb's conception of an Amazon seaway as a cause of Amazonian floral and faunal diversity seems limited.

Räsänen *et al.* consider two possible depositional environments for the sediments they studied (p. 388), fluvial or tidal, and conclude that they are tidal. However, in a tropical fluvial environment such as that in which the Solimões Formation was deposited, periodical flooding of the overbank environment causes alternating mud and sand lenticles such as those described (*1*). Moreover, the north- to southeast-directed paleocurrents and the sediment composition of Andean origin coincide with the transport direction and the sediment composition reported for the paleo-Amazon River (*9*). Furthermore, Räsänen *et al.* relate the timing of the presumed seaway to the Late Serravallian, which is Middle Miocene (*12*), and not to Late Miocene, as the title of their report suggests. The base of the Late Miocene [~10.4 Ma (million years ago)] represents the largest drop in sea level in the entire Miocene; thus it is not likely that a marine ingression would occur. Moreover, during the Late Serravallian, the maximum sea level rise was estimated at about 50 m, whereas at the base of the Serravallian (~14.2 Ma), the maximum sea level rise was estimated at 150 m (*13*). If there was a marine ingression it would be thus more understandable if it occurred in this interval. Indeed, there is evidence elsewhere in Amazonia (*8–10*) of a base Serravallian marine ingression, on the basis of the presence of marine fossils and palynomorphs (*14*). In addition to this, the connection between the paleo-Amazon and the Atlantic was well established during the Late Miocene. The clastic sediments on the Guyana shelf and in the Amazon cone are evidence of the Amazon-Atlantic connection (*15–17*). Therefore, a Late Miocene marine connection between the Caribbean and the southern Atlantic at this same time is highly unlikely.

The Late Miocene sediments studied by Räsänen *et al.* are most likely fluvial, not tidal, and were probably deposited by the ancestral Amazon River. There were marine ingressions in Amazonia during the Early and Middle Miocene, but not in the Late Miocene. Moreover, during the Early and Middle Miocene, the connection between Amazonia and the sea had a more modest character than the seaway postulated by Räsänen *et al.* Their model might be applicable to the Cretaceous (for which marine deposits are well known to exist in the eastern Andes and in the foreland basins), but it is not suitable for the Miocene paleogeography.

Carina Hoorn*
Hugo de Vries Laboratory, University of Amsterdam, Amsterdam, Netherlands

*Present address: XEM/3, Petroleum Development, Oman, Post Office Box 81, Muscat 113, Sultanate of Oman